



Published in final edited form as:

*Biochim Biophys Acta*. 2016 January ; 1860(1 0 0): 287–298. doi:10.1016/j.bbagen.2015.05.017.

## $\beta$ A3/A1-crystallin and persistent fetal vasculature (PFV) disease of the eye\*

J. Samuel Zigler Jr.<sup>a</sup>, Mallika Valapala<sup>a</sup>, Peng Shang<sup>a,b</sup>, Stacey Hose<sup>a</sup>, Morton F. Goldberg<sup>a</sup>, and Debasish Sinha<sup>a,\*</sup>

<sup>a</sup>Wilmer Eye Institute, The Johns Hopkins University School of Medicine, Baltimore, MD, USA

<sup>b</sup>Department of Ophthalmology of Shanghai Tenth Hospital and Tongji Eye Institute, Tongji University School of Medicine, Shanghai, China

### Abstract

**Background**—Persistent fetal vasculature (PFV) is a human disease in which the fetal vasculature of the eye fails to regress normally. The fetal, or hyaloid, vasculature nourishes the lens and retina during ocular development, subsequently regressing after formation of the retinal vessels. PFV causes serious congenital pathologies and is responsible for as much as 5% of blindness in the United States.

**Scope of review**—The causes of PFV are poorly understood, however there are a number of animal models in which aspects of the disease are present. One such model results from mutation or elimination of the gene (*Cryba1*) encoding  $\beta$ A3/A1-crystallin. In this review we focus on the possible mechanisms whereby loss of functional  $\beta$ A3/A1-crystallin might lead to PFV.

**Major conclusions**—*Cryba1* is abundantly expressed in the lens, but is also expressed in certain other ocular cells, including astrocytes. In animal models lacking  $\beta$ A3/A1-crystallin, astrocyte numbers are increased and they migrate abnormally from the retina to ensheath the persistent hyaloid artery. Evidence is presented that the absence of functional  $\beta$ A3/A1-crystallin causes failure of the normal acidification of endolysosomal compartments in the astrocytes, leading to impairment of certain critical signaling pathways, including mTOR and Notch/STAT3.

**General significance**—The findings suggest that impaired endolysosomal signaling in ocular astrocytes can cause PFV disease, by adversely affecting the vascular remodeling processes essential to ocular development, including regression of the fetal vasculature. This article is part of a Special Issue entitled Crystallin Biochemistry in Health and Disease.

### Keywords

Astrocytes;  $\beta$ A3/A1-crystallin; Fetal/hyaloid vasculature; Notch/STAT signaling; PI3K/Akt/mTOR signaling; Vascular remodeling

\*This article is part of a Special Issue entitled Crystallin Biochemistry in Health and Disease.

\*Corresponding author at: The Wilmer Eye Institute, The Johns Hopkins University School of Medicine, Baltimore, MD 21287, USA. Debasish@jhmi.edu (D. Sinha).

Persistent fetal vasculature (PFV) is a human disease that results from failure of the fetal vasculature of the eye to regress normally [1]. We have developed novel animal models [2,3] that mimic clinical signs of human PFV, a potentially blinding childhood disease, for which there are limited treatment options at the present time. These models result from mutation or knockout of  $\beta$ A3/A1-crystallin, an abundant lens protein that is also expressed in astrocytes. In this review, we focus on how loss of functional  $\beta$ A3/A1-crystallin in ocular astrocytes may potentiate PFV disease.

## 1. Fetal vasculature of the eye

In mammals, the fetal vasculature of the eye includes the hyaloid artery, which very early in development enters the eye from the retinal fissure and grows into the vitreous chamber; there it produces a network of vessels (vasa hyaloidea propria) throughout the vitreous and blankets the posterior and anterior aspects of the lens (posterior and anterior tunica vasculosa lentis). Together with the vessels of the pupillary membrane, which cover the anterior surface of the lens and iris, these structures constitute the fetal or hyaloid vasculature, which nourishes the developing lens and retina [4] (Fig. 1). When the retinal vasculature begins to form, the fetal vasculature regresses, normally disappearing completely in the human by the 8th month of gestation and by the end of the 3rd postnatal week in rats and mice [5–7]. The regression of vessels occurs via vascular remodeling, an active process of structural alterations that involves several critical mediators [8]; our studies to date suggest that  $\beta$ A3/A1-crystallin is one of the factors involved in the physiological regulation of hyaloid vessel regression [2–4]. The possibility that  $\beta$ A3/A1-crystallin may have a role in vascular remodeling is important, because such remodeling is fundamental to normal ocular development, as well as to the pathogenesis of numerous diseases.

## 2. Persistent fetal vasculature (PFV)

Persistent fetal vasculature is a human disease that results from failure of the fetal vasculature to regress normally. Failure of all or part of these vessels to regress can lead to serious congenital pathologies [1]. The defects include congenitally small eye, cataract, glaucoma, intravitreal fibrovascular tissue and/or hemorrhage, and retinal detachment.

PFV has been reported in other mammalian species, particularly in dogs [9–11] and in genetic mouse models [12–20]. Studies with these animals have helped immensely with our current understanding of the disease.

The regulatory mechanisms responsible for fetal vascular regression remain obscure, as does the underlying cause of failure of regression. The exact prevalence of PFV is unknown; however, a study on childhood blindness and visual loss in the United States showed that PFV accounts for about 5% of all cases of blindness.

## 3. $\beta$ A3/A1-crystallin and persistent fetal vasculature

A connection between the lens protein  $\beta$ A3/A1-crystallin and PFV arose initially because of the identification of *Cryba1* (the gene encoding  $\beta$ A3/A1-crystallin) as the gene that is mutated in the Nuc1 rat [21]. Nuc1 is a spontaneous mutation in the Sprague–Dawley rat in

which 27 base pairs are inserted into Exon 6, leading to the loss of a highly conserved glycine and its replacement by 10 new amino acid residues. Rats homozygous for this mutation have a complex eye phenotype that frequently includes persistence of the complete fetal vasculature [2]. *Cryba1* produces 2 polypeptides,  $\beta$ A3-crystallin and  $\beta$ A1-crystallin, which are translated from the same mRNA using alternative initiation sites [22]. The 2 polypeptides are identical in primary sequence, except that  $\beta$ A3-crystallin has an additional 17 amino acid residues at its amino terminus. At present it is not known whether the 2 polypeptides have distinct functions.  $\beta$ A3- and  $\beta$ A1-crystallins (hereafter referred to collectively as  $\beta$ A3/A1-crystallin) are both abundantly expressed in the lens where they associate as dimers or higher oligomers with the 5 other homologous  $\beta$ -crystallin polypeptides to form native molecules ranging in mass from about 50 kD to about 200 kD [23]. The  $\beta$ -crystallins, along with the evolutionarily related  $\gamma$ -crystallins and the unrelated  $\alpha$ -crystallins, constitute over 90% of the total protein of the lens. Together, these are the structural proteins that form the very dense and highly ordered protein matrix of the lens, upon which the refractivity and transparency critical to lens function depend [23]. The importance of  $\beta$ A3/A1-crystallin to lens function is demonstrated by the fact that mutations in *Cryba1* have been shown in both animal models and in human patients to lead to cataract (loss of transparency of the lens) [24,25].

Long thought to be proteins expressed only in the lens,  $\alpha$ -crystallins and the  $\beta/\gamma$ -crystallin superfamily are now known to pre-date the evolution of the lens [26]. Further, these proteins are not lens-specific and have cellular functions in addition to their structural roles in the lens. The  $\alpha$ -crystallins are members of the small heat shock protein family; they are expressed in a wide range of tissues and cell types where they have the functions characteristic of small heat shock proteins [27]. For members of the  $\beta/\gamma$ -crystallin superfamily, the situation is less clear. While they are expressed outside of the lens, they are found predominately in ocular tissues, where their functions are poorly understood. For  $\beta$ A3/A1-crystallin specifically, expression in the eye appears to be limited to retinal pigmented epithelial cells, astrocytes, and some retinal ganglion cells, in addition to the lens [28]. Outside of the eye,  $\beta$ A3/A1-crystallin has been found only in the astrocytes of the brain [21], where studies on possible functions have not been conducted to date.

With regard to the association of  $\beta$ A3/A1-crystallin and PFV, our laboratory has produced evidence that abnormalities in retinal and optic nerve astrocytes are responsible, at least in part, for the PFV observed in the Nuc1 rat [2,4] and in genetically engineered mouse models that have been generated to study the possible functions of  $\beta$ A3/A1-crystallin [3]. Under normal physiological conditions, the hyaloid artery regresses by P (postnatal day) 21 in rodents (Fig. 2a). In contrast, Nuc1 rats at P35 displayed persistence of the hyaloid artery (Fig. 2b) and the pupillary membrane (Fig. 2c, arrow), iris hyperplasia (Fig. 2c, arrowhead), disrupted lens (Fig. 2c) and dragging and folding of the peripheral retina (Fig. 2d).

In rats homozygous for the Nuc1 mutation, astrocytes were shown to migrate abnormally out of the retina and to ensheath the retained hyaloid artery [2,4]. They also had increased expression of aquaporin-4 (AQP4) (Fig. 3), a water channel known to facilitate cell migration [29,30]. It has been elegantly shown that deletion of AQP4 slows astrocyte migration and is associated with delayed glial scar formation [29]. Recently, we found that

Author Manuscript

animals lacking  $\beta$ A3/A1-crystallin in the RPE had markedly decreased levels of certain Rho GTPases (unpublished), cell signaling factors previously shown to activate cell migration [31]. Similarly, in transgenic mice over-expressing the mutant (Nuc1) form of  $\beta$ A3/A1-crystallin, some animals were found to retain the hyaloid artery abnormally, and astrocytes were again associated with the artery [3]. Finally, in current work involving mice in which  $\beta$ A3/A1-crystallin has been knocked out globally, PFV has been found to be present in some individuals (unpublished). Therefore, in the absence of functional  $\beta$ A3/A1-crystallin, astrocytes in the eye are abnormal, leading to defects in vascular remodeling. Our previous studies demonstrated such defects in the remodeling required to develop the mature retinal vasculature, as well as the remodeling that underlies the regression of the fetal vasculature [2,4]. Notably, in human cases of PFV, astrocytes may also ensheath the retained hyaloid artery (Fig. 4).

Author Manuscript

In the retina, astrocytes have multiple functions that include regulation of blood vessel structure and function [32]. They migrate ahead of the vessels (vascular “front”), and are thus in a position to respond to local environmental signals [33]. In a transwell migration assay, Nuc1 astrocytes showed increased migration compared to wild type cells (Fig. 5a). They also exhibited an increased rate of proliferation in an MTS (3-(4, 5-dimethylthiazol-2-yl)-5-(3-carboxymethoxyphenyl)-2-(4-sulfophenyl)-2H-tetrazolium) assay (Fig. 5b). Although all cells associated with the vasculature may participate in the remodeling process, astrocytes may play a particularly important part, because they are capable of sensing changes within their immediate milieu.

Author Manuscript

Astrocytes are known to be oxygen sensors, an attribute which may be critical, both to hyaloid regression and retinal vascular development. During the vascular remodeling that occurs during hyaloid regression, HIF-1 $\alpha$  in the astrocytes activates macrophage migration inhibitory factor (MIF), thereby recruiting macrophages that earlier were shown to play a significant role in the normal regression of the hyaloid vasculature [34]. Persistence of the hyaloid vasculature was reported in transgenic mice where macrophages were disrupted by directed expression of diphtheria toxin, using macrophage-specific promoter elements [35]. Our data show ED1-positive macrophages surrounding the stump of the hyaloid artery, both in wild type (involuting) and Nuc1 (not involuting) eyes at 21 days of age (Fig. 6). Our data also suggested that the number of macrophages is proportional to the length of the persistent artery [2].

Author Manuscript

While the specific function(s) of  $\beta$ A3/A1-crystallin in non-lens cell types is not well understood, our recent studies indicate that the protein is essential in the acidification of lysosomes in both astrocytes and RPE cells [36,37]. It also regulates important signaling pathways in both cell types during both health and disease [37–41]. Studies on rat RPE demonstrated by immuno-electron microscopy that in normal tissue  $\beta$ A3/A1-crystallin strongly localizes to the lysosomes, whereas in the RPE of Nuc1 homozygous animals the mutant form of the protein is expressed, but not trafficked to the lysosomes [36]. Lysosomal-mediated clearance of phagosomes and autophagosomes from the RPE cells of the mutant animals is markedly impaired [38]. Subsequent studies on primary cultures of optic nerve astrocytes demonstrated that impairment of endolysosomal function also occurs in these cells when  $\beta$ A3/A1-crystallin is absent or mutated [37].

Although not specifically noted in the published accounts, several other mouse models that exhibit PFV also appear to have astrocytes associated with the persistent hyaloid artery [42–44]. In addition, eyes from Frizzled 5 knockout mice show PFV and increased number of astrocytes [45]. In many of these mouse models, the hyaloid vessels likely persist to compensate for the absence, or decreased number, of retinal vessels [6]. In contrast, in Nuc1 homozygous rats the initial network of retinal vessels does form, but there appears to be a defect in the remodeling process necessary to produce a mature vasculature [21,46]. Further, Nuc1 exhibits inhibition of the normal regression of the entire fetal intraocular vasculature and not just part of it, as reported in previous mouse models. To date, our data suggest that developmental abnormalities in Nuc1 astrocytes lead to abnormal migration and association with the hyaloid artery. This may inhibit the normal programmed regression of the fetal vasculature and thereby be involved in the pathogenesis of PFV disease [2,4]. Several lines of evidence link the astrocyte defects associated with the loss of  $\beta$ A3/A1-crystallin to altered activity of signal transduction pathways. The next section of this review focuses on signaling pathways that may have roles in persistence of the fetal vasculature when  $\beta$ A3/A1-crystallin is mutated or absent.

#### 4. $\beta$ A3/A1-crystallin and signaling in astrocytes

Cell death and its regulation is central to vascular remodeling, including normal regression of the hyaloid vasculature. Our studies using the Nuc1 model have shown that  $\beta$ A3/A1-crystallin plays a major role in the anoikis-mediated programmed cell death (PCD) process in astrocytes [39]. Anoikis is a form of PCD initiated by loss of cell anchorage [47,48]. We have previously shown that Bit1 (Bcl-2 inhibitor of transcription-1), a known regulator of anoikis, is expressed in normal optic nerve astrocytes, suggesting that anoikis functions as a form of PCD for astrocytes (Fig. 7). Staining for Bit-1 was more intense in the optic nerve astrocytes from Nuc1 animals as compared to wild type, suggesting that Bit-1-induced anoikis is upregulated in the Nuc1 optic nerve astrocytes. To provide further support to these observations, we studied the anoikis pathway in cultured post natal day 2 wild type and Nuc1 optic nerve astrocytes. Anoikis was induced by plating the cells on low-attachment poly-2-hydroxyethyl methacrylate (poly-HEMA) plates [39]. Wild type astrocytes formed small, sparse aggregates, whereas Nuc1 astrocytes formed large, dense aggregates. Furthermore, there was a 20% increase in cell death in wild type astrocytes in cells grown for 3 days on poly-HEMA plates and greater than 2 fold increase in cell death after 5 days in wild type astrocytes grown on poly-HEMA, as compared to Nuc1 astrocytes (Fig. 8a). A significant increase in proliferation was also observed in Nuc1 cells when they were cultured for 5 days on poly-HEMA plates followed by normal culture for 7 days (Fig. 8b). In addition, we also observed a significant increase in phosphorylated PKD [49], an upstream activator of Bit-1, in Nuc1 astrocytes compared to wild type astrocytes, whereas the levels of cleaved caspase-3 and apoptosis-inducing factor (AIF), mediators involved in the normal apoptotic pathway, remained unchanged [39]. Knockdown of Bit-1 in wild type astrocytes caused a significant reduction in cell death when anoikis was induced (Fig. 8c). Upon investigating possible signaling mechanisms regulating anoikis in astrocytes, we found that PI3K (phosphatidylinositol-3-kinase), AKT and mTOR (mechanistic target of rapamycin) are phosphorylated and activated more in Nuc1 astrocytes than in wild type when anoikis is

induced (Fig. 9). Moreover, we also observed increased phosphorylation and activation of ERK1/2 (extracellular signal-regulated kinases 1/2) and ILK (integrin-linked kinase) in anoikis-induced Nuc1 astrocytes compared to wild type astrocytes (Fig. 9). These data indicated that anoikis is inhibited and cell survival increased in the Nuc1 astrocytes [39]. To further investigate the signaling mechanisms involved, Nuc1 astrocytes were treated with the mTOR inhibitor, rapamycin, alone or in combination with the ERK inhibitor FR180204. A decrease in proliferation was observed. Under anoikis conditions, these inhibitors, either alone or in combination, significantly increased cell death in Nuc1 cells compared to wild type cells [39]. These findings demonstrate that loss of functional  $\beta$ A3/A1-crystallin impairs the anoikis-mediated cell death process in astrocytes. This may lead to an excess number of astrocytes and contribute to the failure of the hyaloid vasculature to regress normally.

Our studies on the Nuc1 rat retina have also revealed severe abnormalities in the structure of the astrocyte template and in the remodeling of the retinal vasculature [21,37,46]. Since the astrocyte template is believed to direct the formation of retinal vessels, we have investigated the signaling mechanisms by which  $\beta$ A3/A1-crystallin might regulate formation of this template. Retinal vascular development is an intricate process involving multiple signaling pathways. One of the most important of these is the Notch pathway, which is involved in patterning and maintenance of vascular homeostasis [50]. The Notch family receptors are large single-pass type I transmembrane proteins [51]. In mammals, four Notch receptors (Notch1–4) have been identified. Our studies on the expression of Notch receptors in optic nerve astrocytes have shown elevated levels of Notch1 receptor in the Nuc1 astrocytes compared to wild type [37]. We have also demonstrated that wild type and Nuc1 astrocytes express similar levels of the Notch ligand, Jagged1. Since both the receptor, Notch1, and the ligand, Jagged1, are expressed in these cells [52], we believe that Notch signaling could be involved in astrocyte template formation.

We determined the level of expression of the activated form of Notch, NICD (Notch intracellular domain), in wild type and Nuc1 astrocytes [37]. Upon ligand binding and activation, NICD is generated by proteolytic cleavage of the Notch receptor. A series of cleavages within the Notch receptor, mediated first by a disintegrin and metalloproteinase (ADAM) and then by  $\gamma$ -secretase, results in the generation of NICD [53,54]. After NICD is formed in the cytosol, it translocates to the nucleus, interacts with RBP-J (recombination signal sequence-binding protein for immunoglobulin kappa J region), and activates transcription of Notch downstream targets, Hey1 and Hes1 [55]. Our immunoblotting studies revealed a significant decrease in the expression of NICD in Nuc1 astrocytes compared to wild type astrocytes [37]. These studies suggest that the proteolytic processing leading to the generation of NICD is disrupted in Nuc1 astrocytes.

Hence, we investigated the proteolytic activity of  $\gamma$ -secretase, the enzyme that catalyzes the final cleavage of the Notch receptor to generate NICD. Previous studies have demonstrated that  $\gamma$ -secretase activation is dependent upon the low pH environment of the endolysosomal compartments [56–58]. In order to determine the localization and activity of  $\gamma$ -secretase, we performed subcellular fractionation on cultured astrocytes to isolate endosomes, lysosomes and Golgi fractions [37]. After confirming the purity of these fractions by immunoblotting, we determined the activity of  $\gamma$ -secretase in each fraction. Our results showed significantly

reduced  $\gamma$ -secretase activity in the endolysosomal fractions (3, 4 and 5 = lysosomal fractions; 6, 7 and 8 = endosomal fractions) isolated from the Nuc1 astrocytes, as compared to wild type astrocytes (Fig. 10a). The activity of  $\gamma$ -secretase was similar in the Golgi fractions (9 and 10) from wild type and Nuc1 astrocytes. Near normal activity could be restored in cultured Nuc1 homozygous astrocytes by overexpression of  $\beta$ A3/A1-crystallin (Fig. 10b). In addition, astrocytes isolated from *Cryba1* floxed mice and transduced with adenoviral vectors expressing *Cre*-recombinase to ablate  $\beta$ A3/A1-crystallin, showed decreased  $\gamma$ -secretase activity, which could be rescued by subsequent over-expression of  $\beta$ A3/A1-crystallin [37].

Since our studies have shown that  $\gamma$ -secretase activity is inhibited in the Nuc1 astrocytes and because  $\gamma$ -secretase activation is dependent upon the acidic environment of the lysosomal lumen, we asked whether endolysosomal acidification is dysregulated in these cells. Lysosomes were isolated from wild type and Nuc1 astrocytes and the activity determined for the lysosomal proton pump, vacuolar-type  $H^+$ -ATPase (VATPase), which pumps protons into the lysosomal lumen to effect acidification [59–62]. The isolated lysosomes were incubated with acridine orange, and exogenous ATP was added to activate V-ATPase [37]. Accumulation of protonated acridine in the lysosomal lumen was measured by the resultant fluorescence which was used to estimate the activity of V-ATPase [37]. Upon addition of ATP, we observed significantly more acridine orange in wild type lysosomes than in lysosomes isolated from Nuc1 astrocytes (Fig. 11a, b). The activity of V-ATPase could be rescued in the Nuc1 astrocytes upon overexpression of  $\beta$ A3/A1-crystallin. These results suggest a potential role of  $\beta$ A3/A1-crystallin in regulating lysosomal acidification via V-ATPase [37]. To confirm that the Nuc1 lysosomes were not acidified to the normal extent, we measured endolysosomal pH in wild type and Nuc1 astrocytes. We observed that the average endolysosomal pH was 4.5 in wild type cells, whereas in the Nuc1 cells it was increased to 5.7. Furthermore, the increase in the lysosomal pH in the Nuc1 cells was reversed by overexpression of  $\beta$ A3/A1-crystallin (Fig. 11c). These results indicated that decreased V-ATPase activity in the Nuc1 astrocytes leads to elevated lysosomal pH.

Previous studies have suggested that proper acidification of the endolysosomal compartments is essential for normal functioning of the Notch signaling pathway [60,62]. To study the processing of the Notch receptor, wild type and Nuc1 astrocytes were transfected with Myc-tagged full length Notch1 receptor and co-cultured with cells overexpressing Jagged1. Our results show, as expected, that the Myc-tagged Notch1 receptor was largely cleared from the cytosol of wild type astrocytes in 3 h. In the Nuc1 astrocytes, however, the receptor remained in the perinuclear region (Fig. 12a), suggesting dysfunctional degradation of the Notch receptor. To determine whether the receptor accumulates in specific subcellular compartments in the Nuc1 astrocytes, subcellular fractionation was performed. The Notch1 receptor was found to accumulate primarily in fractions corresponding to lysosomes (LAMP-1 positive) and early endosomes (Rab-5 positive). In addition, upon overexpression of  $\beta$ A3/A1-crystallin in the Nuc1 astrocytes, the endolysosomal accumulation of Notch1 was significantly reduced. Subcellular localization by immunofluorescence revealed that  $\beta$ A3/A1-crystallin was present both in the cytosol and the lysosomes [37], however there was significantly less in Nuc1 lysosomes than in

lysosomes from wild type astrocytes. These results were further confirmed by subcellular fractionation and immunoblot analysis. Thus,  $\beta$ A3/A1-crystallin is localized to the lysosomes in astrocytes, and loss of functional  $\beta$ A3/A1-crystallin in Nuc1 causes impairment of lysosomal function [37]. To substantiate this conclusion, we compared the activity of cathepsin D, a representative lysosomal acidic hydrolase, in wild type and Nuc1 astrocytes [37]. Cathepsin D activity was markedly reduced in Nuc1 astrocytes, as would be expected due to the increased pH, and could be rescued by overexpression of  $\beta$ A3/A1-crystallin (Fig. 12b). In summary, our data suggest that  $\beta$ A3/A1-crystallin is localized to the lysosomes and plays a crucial role in acidification, thereby impacting the endolysosomal signaling of the Notch pathway in astrocytes.

Astrocyte-derived VEGF has been shown to be a critical factor in mediating vascular stabilization and remodeling in the developing mammalian eye [63,64]. Since previous studies have suggested that Notch signaling is involved in the temporal and spatial control of VEGF expression [65,66], we investigated the association between Notch and VEGF signaling in astrocytes [41]. Our results showed that the levels of astrocyte-derived VEGF were significantly lower in Nuc1 astrocytes as compared to wild type cells (Fig. 13a). We also showed that the Notch inhibitor, DAPT, significantly reduced the levels of VEGF in both wild type and Nuc1 astrocytes (Fig. 13b). In addition, mouse astrocytes from *Cryba1* floxed mice (*Cryba1*<sup>fl/fl</sup>) were infected with control adeno-virus (Ad CMV eGFP) or with *Cre* recombinase adenovirus (Ad CMV *Cre*-RSV GFP) to attain *Cre*-mediated knockdown of *Cryba1*. The astrocytes in which *Cryba1* was knocked down showed a decrease in VEGF secretion similar to that seen in Nuc1 (Fig. 13c). These results suggested that the Notch signaling pathway played a crucial role in the regulation of astrocyte-derived VEGF in optic nerve astrocytes.

Previous studies have suggested a link between Notch signaling and the determination of cell fate in glial cells, a process involving STAT3 (signal transducers and activators of transcription 3), a transcriptional factor activated downstream of Notch [67–70]. STATs are latent gene regulating proteins, which migrate to the nucleus and regulate gene transcription after they are activated by phosphorylation [67]. STAT3 is activated by binding of Interleukin-6 (IL-6) to the gp130 receptor, which leads to phosphorylation by Janus activated kinase 2 (JAK2) [71]. Upon treatment with IL-6, immunoblotting and ELISA (Fig. 14a) revealed a significant increase in p-STAT3 in wild type astrocytes [41]. STAT3 activation was also inhibited in these cells by Stattic, an inhibitor that prevents activation, dimerization and nuclear translocation of STAT3 [72,73]. In Nuc1 astrocytes, however, treatment with IL-6 resulted in significantly lower activation of STAT3 compared to wild type astrocytes (Fig. 14b).

In order to investigate whether STAT3 might regulate the transcription of *Cryba1*, we used the ENCODE program [74], which identified two potential STAT3 binding sites, one in the promoter and one in intron 2 of *Cryba1* (Fig. 15a). We performed quantitative real time PCR (qRT-PCR) to measure the transcript levels of STAT3 in the presence of IL-6 and Stattic. Our results showed that in wild type astrocytes activation of STAT3 by IL-6 resulted in significant induction of *Cryba1* transcript, an increase that was reduced in the presence of Stattic (Fig. 15b). In Nuc1 astrocytes, however, IL-6 treatment resulted in only a modest



elevation of *Cryba1* transcript compared to wild type astrocytes [41]. Thus, our data provide novel evidence that STAT3 regulates the transcription of *Cryba1* [41]. Based on these studies, we believe that  $\beta$ A3/A1-crystallin regulates several signaling pathways, such as the PI3K/AKT/mTOR and Notch/STAT3 cascades, and thereby plays a crucial role in astrocyte-mediated vascular remodeling in the retina (Fig. 16).

## 5. Perspective

PFV is a disease that leads to blindness or serious loss of vision, with few treatment options at present, in otherwise normal children. In loss and gain-of-function mouse models generated to understand the role of  $\beta$ A3/A1-crystallin in astrocytes, we show that this protein is needed to establish the specific mechanisms and signaling molecules involved in crucial physiological processes of astrocytes. The evidence supports the conclusion that in rodents, abrogation of these normal signaling processes due to loss of  $\beta$ A3/A1-crystallin potentiates PFV. It remains to be determined if mutations in  $\beta$ A3/A1-crystallin can contribute to, or cause, PFV disease in humans. Multiple mutations in *Cryba1* are known to cause autosomal dominant cataracts of various descriptions. These are undoubtedly due to disruption of the “crystallin” function of the proteins, leading to protein aggregation and light scattering in the lens. In studies on experimental animals, effects of  $\beta$ A3/A1-crystallin mutations, other than cataract, have invariably been recessive traits. To date, patients homozygous for *Cryba1* mutations have not been reported. Since  $\beta$ A3/A1-crystallin has been shown to be expressed in the human eye, in cells other than lens fibers (unpublished observations), our animal studies suggest that *Cryba1* mutations could negatively affect these cells (e.g., astrocytes), perhaps contributing to the pathogenesis of PFV. Since PFV is a very complex and heterogeneous condition, we recognize that multiple factors may be involved in the abnormal migration of astrocytes in PFV disease. However, our studies with genetically engineered animal models provide strong evidence that loss of  $\beta$ A3/A1-crystallin will lead to abnormal migration of the astrocytes. The signaling pathways that are impacted by loss of  $\beta$ A3/A1-crystallin in the animal models may provide direction for future studies of the human disease.

## Acknowledgments

The authors would like to acknowledge funding support from the National Institutes of Health: EY019037 (DS), EY019037-S (DS), EY018636 (DS), EY01765 (Wilmer Imaging Core); IPA from National Eye Institute (DS); Research to Prevent Blindness (unrestricted grant to The Wilmer Eye Institute); Wilmer Pooled Professors Fund (DS); Knights Templar Eye Foundation (DS) and Intramural Research Program, National Eye Institute (JSZ). The authors would also like to thank the following for their contributions to the earlier studies leading up to this review: Souvonik Adhya, Mille Arora, Laura Ashaghi, Walid Barbour, Colin Barn-stable, Imran A. Bhutto, Lawrence Brako, Karl W. Broman, Peter Campochiaro, Marisol Cano, Aling Dong, Lijin Dong, Melinda K. Duncan, Charles G. Eberhart, Masoud Ashaei Fard, Robert N. Fariss, Peter Gehlbach, Madhumita Ghosh, Celine Gongora, Rhonda Grebe, William R. Green, Seth Greenbaum, Limin Gu, Sean Hackett, Laszlo Hackler, Jr., James T. Handa, J. Fielding Hejmancik, Andrew Klise, Bo Lei, Woo-Kuen Lo, Gerard A. Luty, Bo Ma, Tanya Malpic-Ilanos, D. Scott McLeod, Avindra Nath, Rachel Neal, Terrence P. O'Brien, Geetha Parthasarathy, Bonnie Patek, W. Gerald Robison, Jr., Paul Russell, Sonia Samtani, Gitanjali Sehrawat, Tanusree Sen, Samhita Sengupta, Yuri Sergeev, Kamaljeet Singh, Walter J. Stark, Olof Sundin, Eric F. Wawrousek, Christine Wilson, Goutong Xu, Fang Yang, Donald J. Zack and Cheng Zhang.

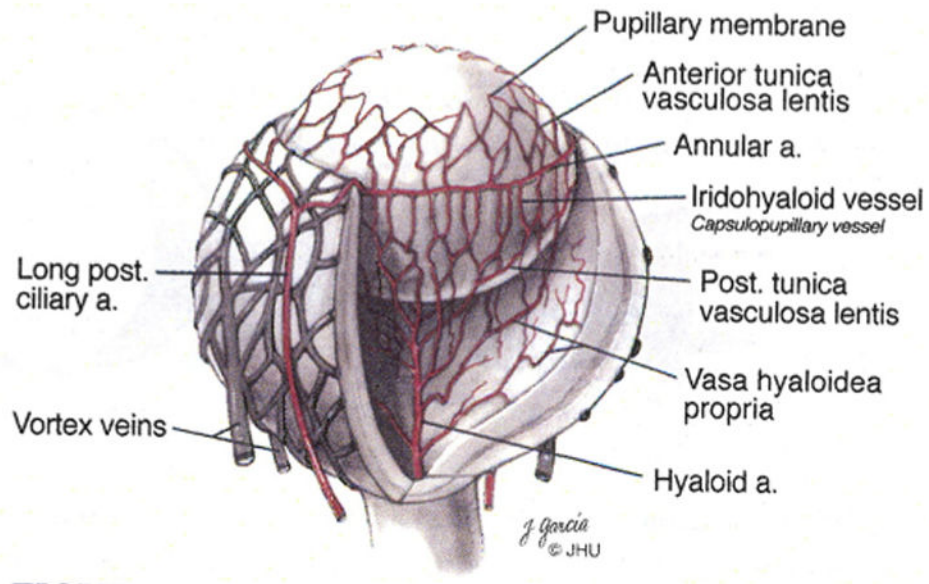
## References

1. Goldberg MF. Persistent fetal vasculature (PFV): an integrated interpretation of signs and symptoms associated with persistent hyperplastic primary vitreous (PHPV). LIV Edward Jackson Memorial Lecture. *Am J Ophthalmol.* 1997; 124:587–626. [PubMed: 9372715]
2. Zhang C, Ashaghi L, Gongora C, Patek B, Hose S, Ma B, Aghsaei-Fard M, Brako L, Singh K, Goldberg MF, Handa JT, Lo WK, Eberhart CG, Zigler JS Jr, Sinha D. A developmental defect in astrocytes inhibits programmed regression of the hyaloid vasculature in the mammalian eye. *Eur J Cell Biol.* 2011; 90(5):440–448. [PubMed: 21354650]
3. Sinha D, Valapala M, Patek B, Bhutto I, Zhang C, Hose S, Fang Y, Cano M, Stark WJ, Luty GA, Zigler JS Jr, Wawrousek E.  $\beta$ A3/A1-crystallin is required for proper astrocytes template formation and vascular remodeling in the retina. *Transgenic Res.* 2012; 21(5):1033–1042. [PubMed: 22427112]
4. Zhang C, Gehlbach P, Gongora C, Cano M, Fariss R, Hose S, Nath A, Green WR, Goldberg MF, Zigler JS, Sinha D. A potential role for  $\beta$ - and  $\gamma$ -crystallins in the vascular remodeling of the eye. *Dev Dyn.* 2005; 234:36–47. [PubMed: 16003775]
5. Ito M, Yoshioka M. Regression of the hyaloid vessels and pupillary membrane of the mouse. *Anat Embryol.* 1999; 200:403–411. [PubMed: 10460477]
6. Saint-Geniez M, D'Amore PA. Development and pathology of the hyaloid, choroidal and retinal vasculature. *Int J Dev Biol.* 2004; 48:1045–1058. [PubMed: 15558494]
7. Zhu M, Provis JM, Penfold PL. The human hyaloid system: cellular phenotypes and inter-relationships. *Exp Eye Res.* 1999; 68:553–563. [PubMed: 10328969]
8. Yancopoulos GD, Davis S, Gale NW, Rudge JS, Wiegand SJ, Holash J. Vascular-specific growth factors and blood vessel formation. *Nature.* 2000:242–248. [PubMed: 11001067]
9. Curtis R, Barnett KC, Leon A. Persistent hyperplastic primary vitreous in the Staffordshire bull terrier. *Vet Rec.* 1984; 115:385. [PubMed: 6506414]
10. Stades FC. Persistent hyperplastic tunica vasculosa lentis and persistent hyperplastic primary vitreous (PHTVL/PHPV) in 90 closely related Doberman Pinschers: clinical aspects. *J Am Anim Hosp Assoc.* 1980; 16:739–751.
11. Stades FC, Boeve MH, van den Brom WE, van der Linde-Sipman JS. The incidence of PHTVL/PHPV in Doberman and the results of breeding rules. *Vet Q.* 1991; 13:24–29. [PubMed: 2021051]
12. Son AI, Sheleg M, Cooper MA, Sun Y, Kleiman NJ, Zhou R. Formation of persistent hyperplastic vitreous in ephrin-A5<sup>-/-</sup> mice. *Invest Ophthalmol Vis Sci.* 2014; 55:1594–1606. [PubMed: 24550361]
13. Hahn P, Lindsten T, Tolentino M, Thompson CB, Bennett J, Dunaief JL. Persistent fetal ocular vasculature in mice deficient in bax and bak. *Arch Ophthalmol.* 2005; 123:797–802. [PubMed: 15955981]
14. Rao S, Chun C, Fan J, Kofron M, Yang MB, Hegde RS, Ferrara N, Copenhagen DR, Lang RA. A direct and melanopsin-dependent fetal light response regulates mouse eye development. *Nature.* 2013; 494:243–247. [PubMed: 23334418]
15. Martin AC, Thornton JD, Liu J, Wang X, Zou J, Jablonski MM, Chaum E, Zindy F, Skapek SX. Pathogenesis of persistent hyperplastic primary vitreous in mice lacking the arf tumor suppressor gene. *Invest Ophthalmol Vis Sci.* 2004; 45:3387–3396. [PubMed: 15452040]
16. Thornton JD, Swanson DJ, Mary MN, Pei D, Martin AC, Pounds S, Goldwitz D, Skapek SX. Persistent hyperplastic primary vitreous due to somatic mosaic deletion of the arf tumor suppressor. *Invest Ophthalmol Vis Sci.* 2007; 48:491–499. [PubMed: 17251441]
17. Reichel MB, Ali RR, D'Esposito F, Clarke AR, Luthert PJ, Bhattacharya SS, Hunt DM. High frequency of persistent hyperplastic primary vitreous and cataracts in p53-deficient mice. *Cell Death Differ.* 1998; 5:156–162. [PubMed: 10200460]
18. Rutland CS, Mitchell CA, Nasir M, Konerding MA, Drexler HC. Microphthalmia, persistent hyperplastic hyaloid vasculature and lens anomalies following overexpression of VEGF-A188 from the alpha-crystallin promoter. *Mol Vis.* 2007; 13:47–56. [PubMed: 17277743]

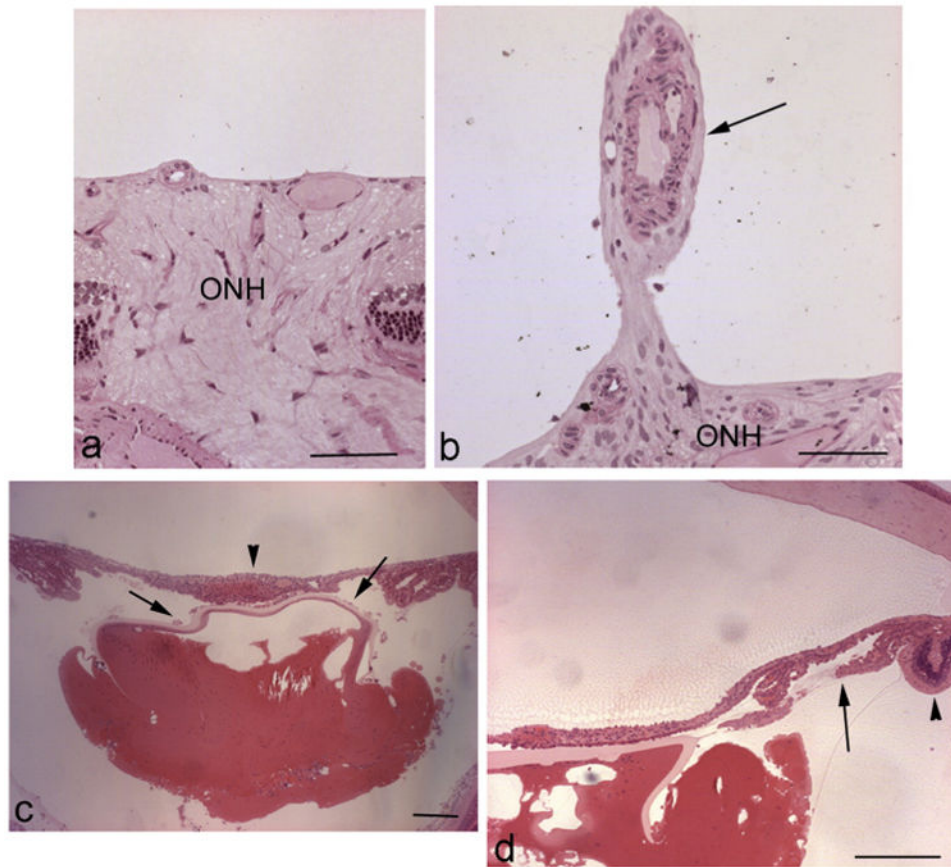
19. Mitchell CA, Rutland CS, Walker M, Nasir M, Foss AJ, Stewart C, Gerhardt H, Konerding MA, Risau W, Drexler HC. Unique vascular phenotypes following over-expression of individual VEGFA isoforms from the developing lens. *Angiogenesis*. 2006; 9:209–224. [PubMed: 17109192]
20. Lahvis GP, Lindell SL, Thomas RS, McCuskey RS, Murphy C, Glover E, Bentz M, Southard J, Bradfield CA. Portosystemic shunting and persistent fetal vascular structures in aryl hydrocarbon receptor-deficient mice. *Proc Natl Acad Sci U S A*. 2000; 97:10442–10447. [PubMed: 10973493]
21. Sinha D, Klise A, Sergeev Y, Hose S, Bhutto IA, Hackler L Jr, Malpic-Ilanos T, Samtani S, Grebe R, Goldberg MF, Hejtmancik JF, Nath A, Zack DJ, Fariss RN, McLeod DS, Sundin O, Broman KW, Luty GA, Zigler JS Jr.  $\beta$ A3/A1-crystallin in astroglial cells regulates retinal vascular remodeling during development. *Mol Cell Neurosci*. 2008; 37:85–95. [PubMed: 17931883]
22. Werten PJJ, Stege GJJ, de Jong WW. The short 5' untranslated region of the  $\beta$ A3/A1-crystallin mRNA is responsible for leaky ribosomal scanning. *Mol Biol Rep*. 1999; 26:201–205. [PubMed: 10532316]
23. Bloemendal H, de Jong W, Jaenicke R, Lubsen NH, Slingsby C, Tardieu A. Ageing and vision: structure, stability and function of crystallins. *Prog Biophys Mol Biol*. 2004; 86:407–485. [PubMed: 15302206]
24. Graw J. Genetics of crystallins: cataract and beyond. *Exp Eye Res*. 2009; 88:173–189. [PubMed: 19007775]
25. Hejtmancik JF. Congenital cataracts and their molecular genetics. *Semin Cell Dev Biol*. 2008; 19:134–149. [PubMed: 18035564]
26. Zigler JS, Sinha D.  $\beta$ A3/A1-crystallin: more than a lens protein. *Prog Retin Eye Res*. 2015; 44:62–85. [PubMed: 25461968]
27. Horwitz J. Alpha-crystallin can function as a molecular chaperone. *Proc Natl Acad Sci U S A*. 1992; 89:10449–10453. [PubMed: 1438232]
28. Parthasarathy G, Ma B, Zhang C, Gongora C, Zigler JS Jr, Duncan MK, Sinha D. Expression of  $\beta$ A3/A1-crystallin in the developing and adult rat eye. *J Mol Histol*. 2011; 42(1):59–69. [PubMed: 21203897]
29. Saadoun S, Papadopoulos MC, Watanabe H, Yan D, Manley GT, Verkman AS. Involvement of aquaporin-4 in astroglial cell migration and glial scar formation. *J Cell Sci*. 2005; 118:5691–5698. [PubMed: 16303850]
30. Auguste KI, Jin S, Uchida K, Yan D, Manley GT, Papadopoulos MC, Verkman AS. Greatly impaired migration of implanted aquaporin-4 deficient astroglial cells in mouse brain toward a site of injury. *FASEB J*. 2007; 21:108–116. [PubMed: 17135365]
31. Höltje M, Hoffmann A, Hofmann F, Mücke C, Grosse G, Van Rooijen N, Kettenmann H, Just I, Ahnert-Hilger G. Role of Rho GTPase in astrocyte morphology and migratory response during in vitro wound healing. *J Neurochem*. 2005; 95:1237–1248. [PubMed: 16150054]
32. Nedergaard M, Ransom B, Goldman SA. New roles for astrocytes: redefining the functional architecture of the brain. *Trends Neurosci*. 2003; 26:523–530. [PubMed: 14522144]
33. Provis JM. Development of the primate retinal vasculature. *Prog Retin Eye Res*. 2001; 20:799–821. [PubMed: 11587918]
34. Kurihara T, Westenskow PD, Krohne TU, Aguilar E, Johnson RS, Friedlander M. Astrocyte pVHL and HIF- $\alpha$  isoforms are required for embryonic-to-adult vascular transition in the eye. *J Cell Biol*. 2011; 195:689–701. [PubMed: 22084310]
35. Lang RA, Bishop MJ. Macrophages are required for cell death and tissue remodeling in the developing mouse eye. *Cell*. 1993; 74:453–462. [PubMed: 8348612]
36. Zigler JS Jr, Zhang C, Grebe R, Sehrawat G, Hackler, Adhya S, Hose S, McLeod DS, Bhutto I, Barbour W, Parthasarathy G, Zack DJ, Sergeev Y, Luty GA, Handa JT, Sinha D. Mutation in the  $\beta$ A3/A1-crystallin gene impairs phagosome degradation in the retinal pigment epithelium of the rat. *J Cell Sci*. 2011; 124(4):523–531. [PubMed: 21266465]
37. Valapala M, Hose S, Gongora C, Dong L, Wawrousek E, Zigler JS, Sinha D. Impaired endolysosomal function disrupts Notch signaling in optic nerve astrocytes. *Nat Commun*. 2013; 4:1629. [PubMed: 23535650]
38. Valapala M, Wilson C, Hose S, Bhutto IA, Grebe R, Dong A, Greenbaum S, Gu L, Sengupta S, Cano M, Hackett S, Xu G, Luty GA, Dong L, Sergeev Y, Handa JT, Campochiaro P, Wawrousek

- E, Zigler JS Jr, Sinha D. Lysosomal-mediated waste clearance in retinal pigment epithelial cells is regulated by Cryba1/ $\beta$ A3/A1-crystallin via V-ATPase-MTORC1 signaling. *Autophagy*. 2014; 10:480–496. [PubMed: 24468901]
39. Ma B, Sen T, Asnaghi L, Valapala M, Yang F, Hose S, McLeod DS, Lu Y, Eberhart C, Zigler JS Jr, Sinha D.  $\beta$ A3/A1-crystallin controls anoikis-mediated cell death in astrocytes by modulating PI3K/AKT/mTOR and ERK survival pathways via the PKD/Bit1 signaling axis. *Cell Death Dis*. 2011; 2:e217. [PubMed: 21993393]
  40. Valapala M, Edwards M, Hose S, Grebe R, Bhutto IA, Cano M, Berger T, Mak TW, Wawrousek E, Handa JT, Luty GA, Samuel Zigler J Jr, Sinha D. Increased lipocalin-2 in the retinal pigment epithelium of Cryba1 cKO mice is associated with a chronic inflammatory response. *Aging Cell*. 2014; 13:1091–1094. [PubMed: 25257511]
  41. Valapala M, Edwards M, Hose S, Hu J, Wawrousek E, Luty GA, Zigler JS Jr, Qian J, Sinha D.  $\beta$ A3/A1-crystallin is a critical mediator of STAT3 signaling in optic nerve astrocytes. *Sci Rep*. 2015; 5:8755. [PubMed: 25736717]
  42. Hurskainen M, Eklund L, Hägg PO, Fruttiger M, Sormunen R, Ilves M, Pihlajaniemi T. Abnormal maturation of the retinal vasculature in type XVIII collagen/endostatin deficient mice and changes in retinal glial cells due to lack of collagen types XV and XVIII. *FASEB J*. 2005; 19:1564–1566. [PubMed: 15976268]
  43. Reneker LW, Overbeek PA. Lens-specific expression of PDGF-A in transgenic mice results in retinal astrocytic hamartomas. *Invest Ophthalmol Vis Sci*. 1996; 37(12):2455–2466. [PubMed: 8933762]
  44. Edwards MM, McLeod DS, Grebe R, Heng C, Lefebvre O, Luty GA. Lama1 mutations lead to vitreoretinal blood vessel formation, persistence of the fetal vasculature, and epiretinal membrane formation in mice. *BMC Dev Biol*. 2011; 11(1):60. [PubMed: 21999428]
  45. Liu C, Nathans J. An essential role for frizzled 5 in mammalian ocular development. *Development*. 2008; 135:3567–3576. [PubMed: 18832390]
  46. Gehlbach P, Hose S, Zhang C, Cano M, Lei B, Barnstable C, Goldberg MF, Zigler S, Sinha D. Developmental abnormalities in the Nucl rat retina: a spontaneous mutation that affects neuronal and vascular remodeling and retinal function. *Neuroscience*. 2006; 137:447–461. [PubMed: 16289888]
  47. Gilmore AP. Anoikis. *Cell Death Differ*. 2005; 12:1473–1477. [PubMed: 16247493]
  48. Chiarugi P, Giannoni E. Anoikis: a necessary death program for anchorage-dependent cells. *Biochem Pharmacol*. 2008; 76:1352–1364. [PubMed: 18708031]
  49. Biliran H, Jan Y, Chen R, Pasquale EB, Ruoslahti E. Protein kinase D is a positive regulator of Bit1 apoptotic function. *J Biol Chem*. 2008; 283:28029–28037. [PubMed: 18703509]
  50. Gridley T. Notch signaling in vascular development and physiology. *Development*. 2007; 134:2709–2718. [PubMed: 17611219]
  51. Lundkvist J, Lendahl U. Notch and the birth of glial cells. *Trends Neurosci*. 2001; 24:492–494. [PubMed: 11506867]
  52. Claxton S, Fruttiger M. Periodic delta-like 4 expression in developing retinal arteries. *Gene Expr Patterns*. 2004; 5:123–127. [PubMed: 15533827]
  53. Andersson ER, Sandberg R, Lendahl U. Notch signaling: simplicity in design, versatility in function. *Development*. 2001; 138:3593–3612. [PubMed: 21828089]
  54. Spasic D, Annaert W. Building  $\gamma$ -secretase: the bits and pieces. *J Cell Sci*. 2008; 121:413–420. [PubMed: 18256384]
  55. Kopan R, Ilagan MX. The canonical Notch signaling pathway: unfolding the activation mechanism. *Cell*. 2009; 137:216–233. [PubMed: 19379690]
  56. Le Borgne R. Regulation of Notch signalling by endocytosis and endosomal sorting. *Curr Opin Cell Biol*. 2006; 18:213–222. [PubMed: 16488590]
  57. Sorkin A, von Zastrow M. Endocytosis and signalling: intertwining molecular networks. *Nat Rev Mol Cell Biol*. 2009; 10:609–622. [PubMed: 19696798]
  58. Vaccari T, Lu H, Kanwar R, Fortini ME, Bilder D. Endosomal entry regulates Notch receptor activation in *Drosophila melanogaster*. *J Cell Biol*. 2008; 180:755–762. [PubMed: 18299346]

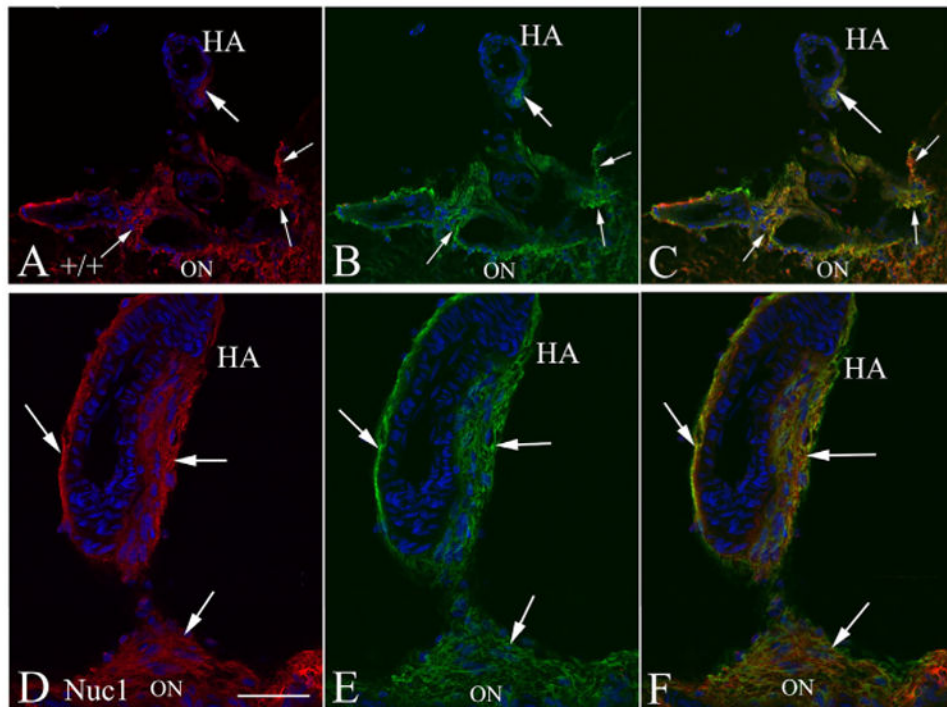
59. Forgac M. Vacuolar ATPases: rotary proton pumps in physiology and pathophysiology. *Nat Rev Mol Cell Biol.* 2007; 8:917–929. [PubMed: 17912264]
60. Yan Y, Deneff N, Schupbach T. The vacuolar proton pump, V-ATPase, is required for notch signaling and endosomal trafficking in *Drosophila*. *Dev Cell.* 2009; 17:387–402. [PubMed: 19758563]
61. Sun-Wada GH, Wada Y, Futai M. Lysosome and lysosome-related organelles responsible for specialized functions in higher organisms, with special emphasis on vacuolar-type proton ATPase. *Cell Struct Funct.* 2003; 28:455–463. [PubMed: 14745137]
62. Vaccari T, Duchi S, Cortese K, Tacchetti C, Bilder D. The vacuolar ATPase is required for physiological as well as pathological activation of the Notch receptor. *Development.* 2010; 137:1825–1832. [PubMed: 20460366]
63. Scott A, Powner MB, Gandhi P, Clarkin C, Gutmann DH, Johnson RS, Ferrara N, Fruttiger M. Astrocyte-derived vascular endothelial growth factor stabilizes vessels in the developing retinal vasculature. *PLoS One.* 2010; 5(7):e11863. [PubMed: 20686684]
64. Gerhardt H, Golding M, Fruttiger M, Ruhrberg C, Lundkvist A, Abramsson A, Jeltsch M, Mitchell C, Alitalo K, Shima D, Betsholtz C. VEGF guides angiogenic sprouting utilizing endothelial tip cell filopodia. *J Cell Biol.* Jun 23.2003 161:1163–1177. [PubMed: 12810700]
65. Jakobsson L, Bentley K, Gerhardt H. VEGFRs and Notch: a dynamic collaboration in vascular patterning. *Biochem Soc Trans.* 2009; 37:1233–1236. [PubMed: 19909253]
66. Suchting S, Freitas C, le Noble F, Benedito R, Bréant C, Duarte A, Eichmann A. The Notch ligand delta-like 4 negatively regulates endothelial tip cell formation and vessel branching. *Proc Natl Acad Sci U S A.* 2007; 104:3225–3230. [PubMed: 17296941]
67. Hirano T, Ishihara K, Hibi M. Roles of STAT3 in mediating the cell growth, differentiation and survival signals relayed through the IL-6 family of cytokine receptors. *Oncogene.* 2000; 19:2548–2556. [PubMed: 10851053]
68. Chenn A. A top-NOTCH way to make astrocytes. *Dev Cell.* 2009; 16:158–159. [PubMed: 19217415]
69. Nagao M, Sugimori M, Nakafuku M. Cross talk between notch and growth factor/cytokine signaling pathways in neural stem cells. *Mol Cell Biol.* 2007; 27:3982–3994. [PubMed: 17371842]
70. Ge W, Martinowich K, Wu X, He F, Miyamoto A, Fan G, Weinmaster G, Sun YE. Notch signaling promotes astroglial gene activation via direct CSL-mediated glial gene activation. *J Neurosci Res.* Sep 15; 2002 69(6):848–860. [PubMed: 12205678]
71. Zhong Z, Wen Z, Darnell JE Jr. Stat3: a STAT family member activated by tyrosine phosphorylation in response to epidermal growth factor and interleukin-6. *Science.* 1994; 264:95–98. [PubMed: 8140422]
72. Schust J, Sperl B, Hollis A, Mayer TU, Berg T. Stattic: a small-molecule inhibitor of STAT3 activation and dimerization. *Chem Biol.* 2006; 13:1235–1242. [PubMed: 17114005]
73. Pan Y, Zhou F, Zhang R, Claret FX. Stat3 inhibitor Stattic exhibits potent antitumor activity and induces chemo- and radio-sensitivity in nasopharyngeal carcinoma. *PLoS One.* 2013; 8:e54565. [PubMed: 23382914]
74. Rosenbloom KR, Sloan CA, Malladi VS, Dreszer TR, Learned K, Kirkup VM, Wong MC, Maddren M, Fang R, Heitner SG, Lee BT, Barber GP, Harte RA, Diekhans M, Long JC, Wilder SP, Zweig AS, Karolchik D, Kuhn RM, Haussler D, Kent WJ. ENCODE data in the UCSC Genome Browser: year 5 update. *Nucleic Acids Res.* 2013; 41(Database issue):D56–D63. [PubMed: 23193274]



**Fig. 1.** Anastomotic relationships of key components of fetal vasculature. During development of the mammalian eye, nourishment of the immature lens, inner retina and vitreous is provided by the hyaloid vascular system, including the pupillary membrane, tunica vasculosa lentis, vasa hyaloidea propria and the hyaloid artery, as shown in this schematic diagram. Adapted with permission from American Journal of Ophthalmology.

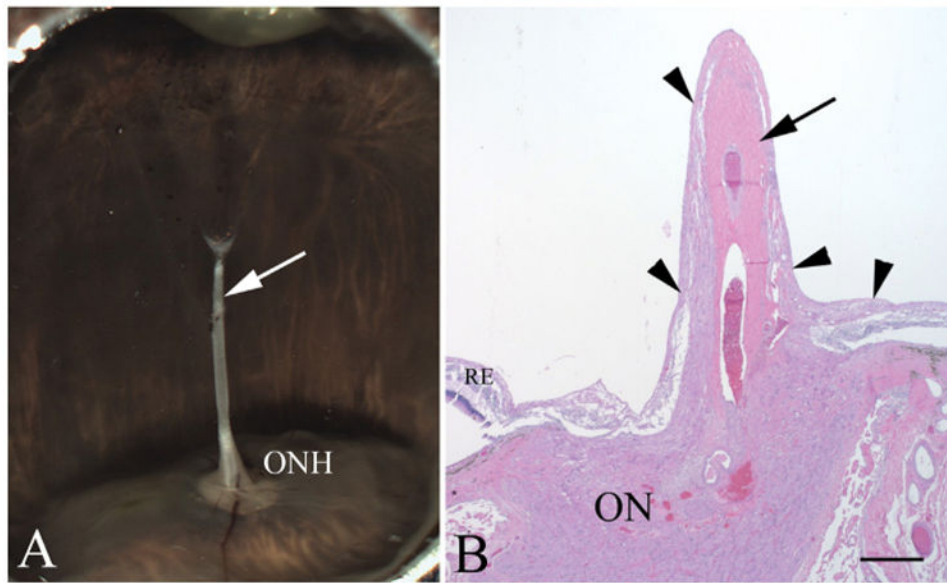


**Fig. 2.** Defective regression of fetal vasculature in *Nuc1* mutant rat. In wild type animals (a), the hyaloid artery had completely regressed by 5 weeks of age, showing a normal optic nerve head (ONH). In *Nuc1* homozygous rats (b), the hyaloid artery and adjacent tissue were still present on the surface of the optic nerve head projecting into the vitreous (arrow). In (c) the pupillary membrane is still evident in the *Nuc1* homozygous animals (arrows). The lens shows abnormal shape and disorganization of structure. In the *Nuc1* homozygote (d), the ciliary process (arrow) is dragged centrally towards the disrupted lens, resulting in traction, which causes peripheral retinal dragging and folding (arrowhead). Scale bars = 50  $\mu\text{m}$ . Adapted with permission from Developmental Dynamics.

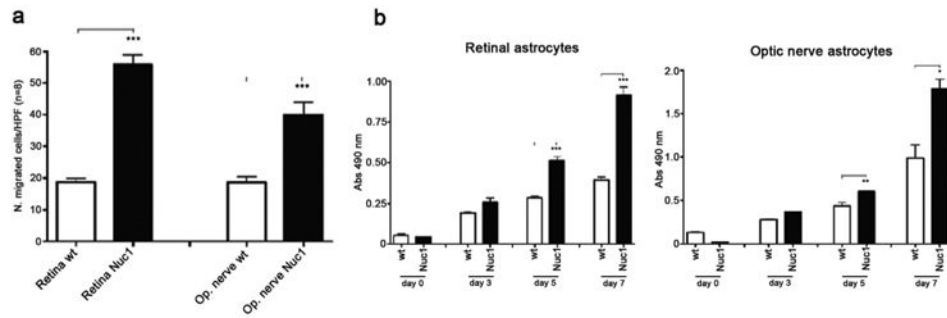


**Fig. 3.** Aquaporin 4 expression by astrocytes at the optic nerve head (ON) and hyaloid artery (HA). Top 3 panels (A–C) are from wild type Sprague–Dawley rats at P20 showing only a remnant of the hyaloid artery (HA) remaining. Staining for both AQP4 (A, red) and GFAP (B, green) is evident in the small cluster of cells around the remnant of the HA (thick arrows) and some cells surrounding the vasculature (thin arrows) at the ON head. The merge (C) shows that some astrocytes in the ON head are AQP4-positive (arrows). Lower panels (D–F) show the P20 Nuc1 homozygote with large intact hyaloid artery. Robust staining for both AQP4 (D) and GFAP (E) is present both at the surface of the optic nerve head and surrounding the hyaloid artery (arrows). The merged image (F) indicates the presence of a dense network of AQP4-positive astrocytes ensheathing the hyaloid artery. Nuclei in all panels are labeled with DAPI (blue). Scale bar = 50  $\mu\text{m}$ ,  $n=5$  wildtype, 5 Nuc1 homozygote. Reproduced with permission from European Journal of Cell Biology.





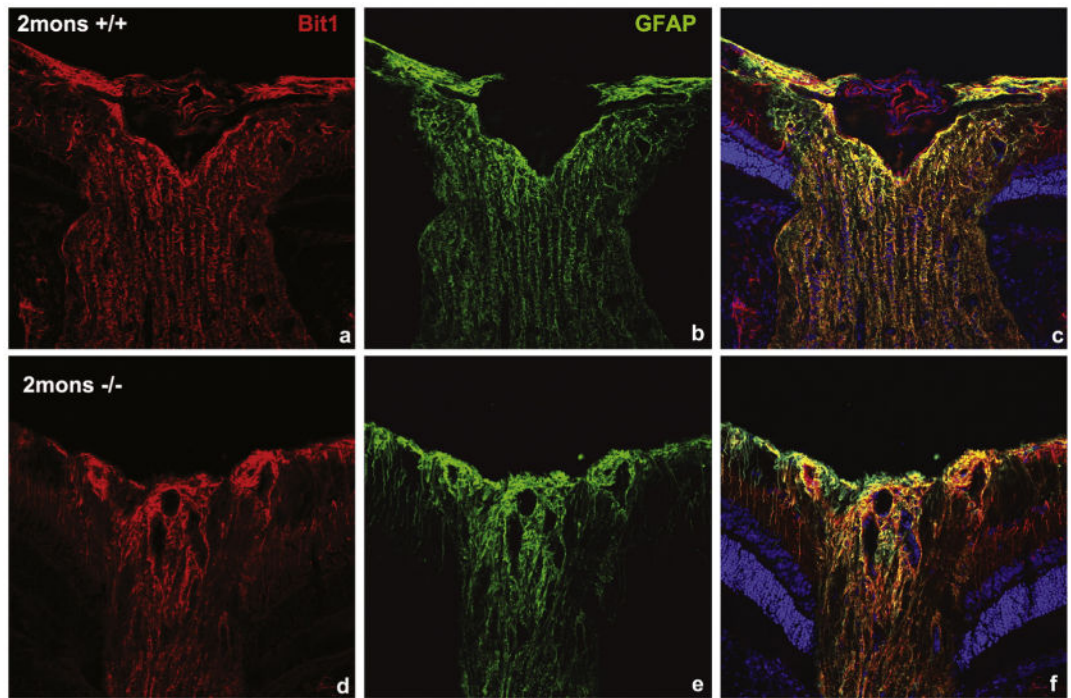
**Fig. 4.** Human PFV: gross morphology and histology. In panel A, the persistent hyaloid artery in an eye from a 30-year old patient is indicated by the arrow and can be seen arising from the optic nerve head (ONH). In panel B, an H&E stained section shows the central persistent hyaloid artery (arrow). Ensheathing the hyaloid artery are multilayered fibrillar cells (arrowheads) that appear to be astrocytes. Scale bar = 100  $\mu$ m. Reproduced with permission from European Journal of Cell Biology.

**Fig. 5.**

Astrocyte migration and proliferation in Nuc1. Astrocytes were cultured from P2 optic nerve and retina and were confirmed to be GFAP-positive. a. For transwell migration assay, cultured astrocytes were incubated for 16 h in the upper chamber of the filter, which was precoated with gelatin. Filters were then stained with hematoxylin, photographed, and the cells migrating to the lower surface of the filter counted. The data shown are the mean ( $\pm$ SEM) of the number of cells counted in 8 different fields from three independent experiments. P-values were calculated between Nuc1 mutant vs. wild type cells using Student t-test (\*\*\*)  $P < 0.0002$ ). b. To measure proliferation, the MTS assay was performed at selected times on cultures of astrocytes from retina and optic nerve of wild type and Nuc1 rats. The data represent the mean value of the absorbance at  $\lambda = 490$  nm, which is proportional to the number of viable cells. Experiments were done in triplicate. P-values were calculated between Nuc1 mutant and wild type cells using Student t-test (\*  $P = 0.03$ , \*\*\*  $P < 0.0007$ ).

Adapted with permission from European Journal of Cell Biology.

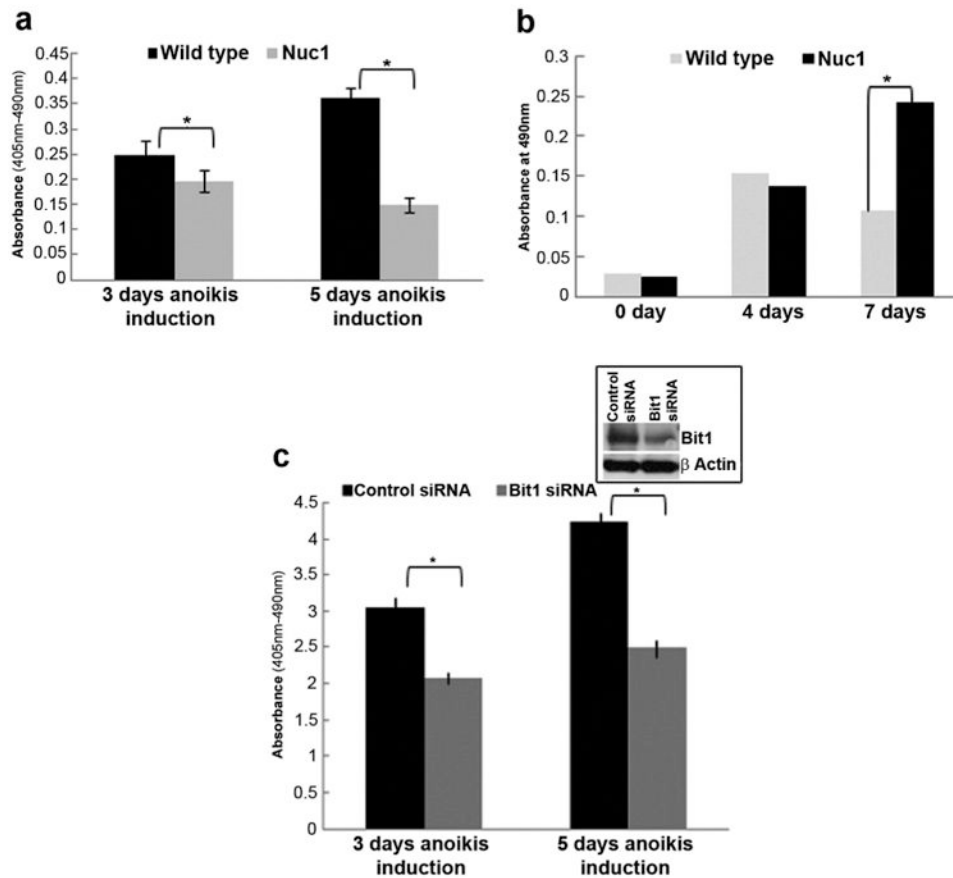




**Fig. 7.**

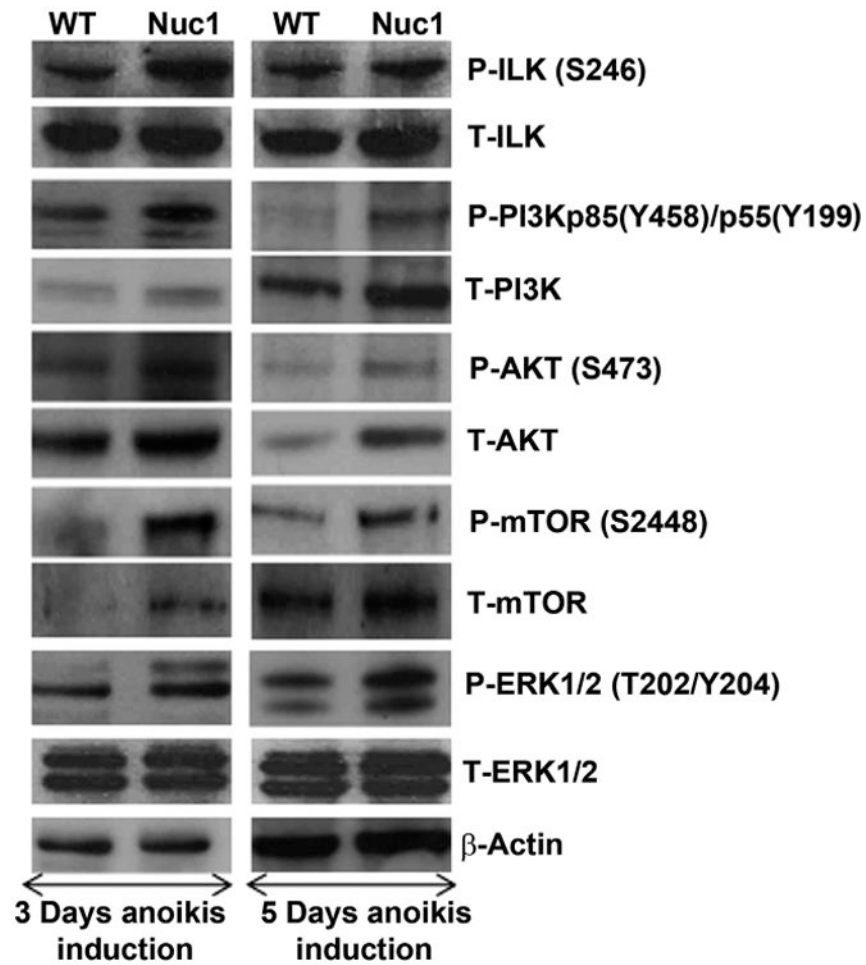
Bit1 expression by astrocytes at the optic nerve head in 2-month old normal and Nuc1 homozygous rats. Confocal microscopy indicated that in wild type optic nerve (panels a, b, c), Bit1 (red) and GFAP (green) are co-expressed (yellow, c). Interestingly, in the Nuc1 homozygous optic nerve (Panels d, e, f) Bit1 (red) and GFAP (green) show more intense co-expression than in wild type.

Adapted with permission from Cell Death and Disease.

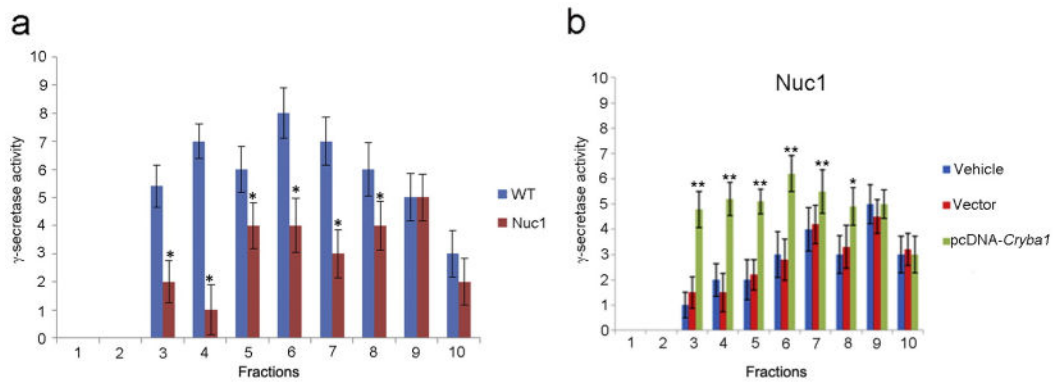
**Fig. 8.**

Effects of anoikis induction on WT and Nuc1 astrocytes. a. Astrocytes were isolated from the optic nerve of wild type and Nuc1 rats and cultured on poly-HEMA plates to induce anoikis. After 5 days on poly-HEMA, Nuc1 astrocytes show significantly higher survival than wild type. Cell death assays performed by Cell Death Detection ELISA<sup>PLUS</sup> kit after 3 and 5 days of anoikis induction show approximately 20% and 50% less cell death in Nuc1 cultures compared to wild type, respectively. Results were plotted as absorbance at 405 nm with a reference wavelength of 490 nm. Experiments were done in triplicate. P-values were calculated using Student's t-test (\*P = 0.001). b. To measure proliferation, the MTS assay was performed with Nuc1 and wild type astrocytes after 5 days of anoikis induction, followed by culture under normal conditions for 0, 4 and 7 days. At 7 days, significant increase in cell proliferation was observed in Nuc1 cultures compared to wild type. The data represent the mean values of absorbance at  $\lambda = 490$  nm, which is proportional to the number of viable cells. Experiments were done in triplicate. P-values were calculated using Student's t-test (\*P = 0.05). c. When Bit1 was knocked-down in wild type astrocytes (western blot in inset) using Bit1 specific siRNA, cell death was decreased following anoikis induction as described above. The data represent the mean values of absorbance at  $\lambda = 490$  nm, which is proportional to the number of viable cells. Experiments were done in triplicate. P-values were calculated using Student's t-test (\*P = 0.05).

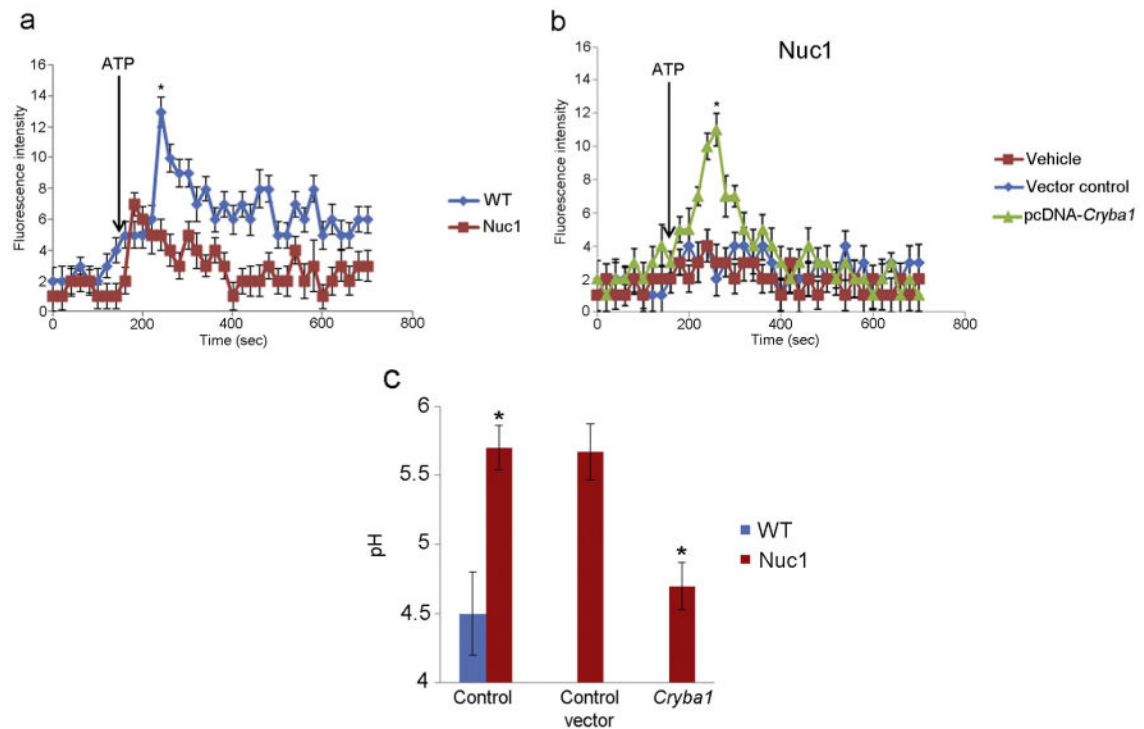
Adapted with permission from Cell Death and Disease.



**Fig. 9.** Signaling pathways in WT and Nuc1 astrocytes. To identify pathways activated in the wild type and the Nuc1 astrocytes after anoikis induction, western-blotting analyses were performed for total and phospho PI3K, total and phospho ILK, total and phospho AKT, total and phospho mTOR, total and phospho ERK1/2 with  $\beta$ -actin as loading control. After 3 and 5 days of anoikis induction, Nuc1 astrocytes show a robust increase in the phosphorylated (activated) forms of PI3K, AKT, mTOR, ILK and ERK1/2 compared to wild type. Adapted with permission from Cell Death and Disease.

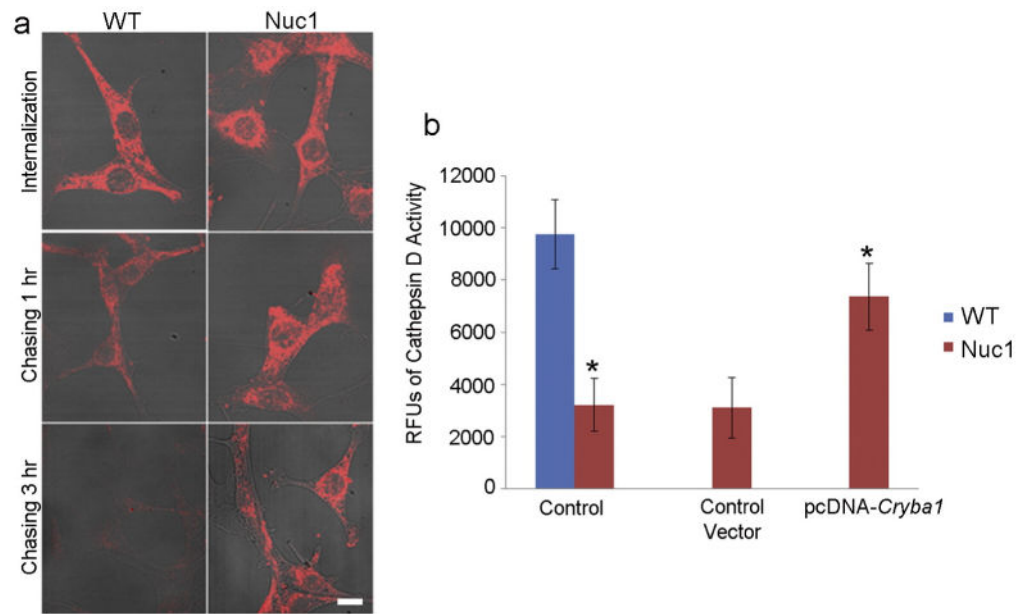
**Fig. 10.**

$\gamma$ -Secretase activity in WT and Nuc1 astrocytes. Post-mitochondrial supernatants from WT and Nuc1 astrocytes were layered on 2.5–30% iodixanol gradients and subjected to ultracentrifugation. Western blots identified LAMP1-positive lysosomes in fractions 3, 4, and 5; Rab5-positive endosomes in fractions 6, 7, and 8; and Golgi in fractions 9 and 10 [37]. a. ELISA was performed to quantify  $\beta$ -amyloid (A $\beta$ 40), which is produced by the action of  $\gamma$ -secretase, after incubating above fractions overnight at 37 °C, with or without L-685,458 ( $\gamma$ -secretase inhibitor). In WT astrocytes (blue),  $\gamma$ -secretase activity, as measured by A $\beta$ 40 level, was detected in all fractions, with the Golgi fractions (9 and 10) having somewhat lower activity. In Nuc1 astrocytes (red),  $\gamma$ -secretase activity was significantly decreased (approximately 50%) in the endolysosomal compartments (fractions 3–8), whereas the activity in Golgi was not significantly different from WT. b. Over-expression of  $\beta$ A3/A1-crystallin in astrocytes cultured from Nuc1 rats rescued  $\gamma$ -secretase activity in endolysosomal compartments, while empty vector had no effect (relative to vehicle). Statistical analysis was performed by a two-tailed Student's t-test: \*P < 0.05. \*\*P < 0.01. Adapted with permission from Nature Communications.

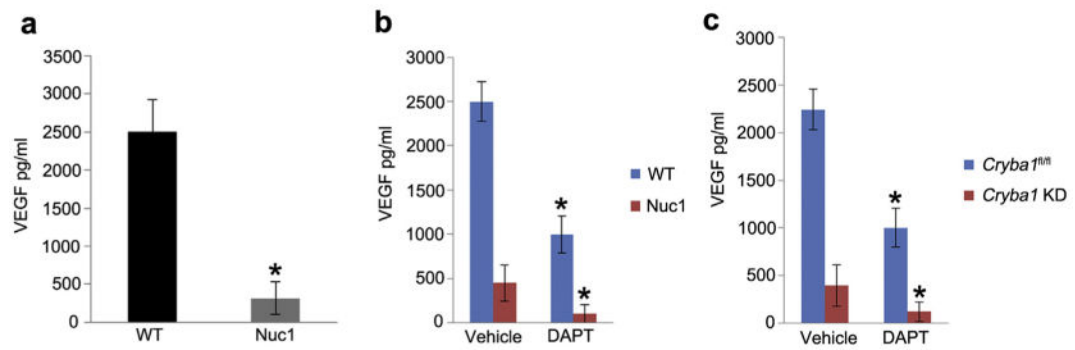
**Fig. 11.**

Impaired V-ATPase activity in astrocytes lacking functional  $\beta$ A3/A1-crystallin. a. V-ATPase activity was measured by acridine orange fluorescence in WT and Nuc1 astrocytes after intravesicular  $H^+$  uptake was initiated by the addition of Mg-ATP. Increase in acridine orange fluorescence (V-ATPase activity) upon addition of ATP was significantly greater in WT astrocytes than in Nuc1 astrocytes. b. In Nuc1 astrocytes, over-expression of  $\beta$ A3/A1-crystallin rescued activity to N80% of normal level (\* $P = 0.020$ ). Empty vector had no effect. c. Measurement of endolysosomal pH in WT and Nuc1 astrocytes was performed using a fluid phase fluorescent probe, FITC-dextran. 3 h after incubation of WT and Nuc1 astrocytes with FITC-dextran the fluorescence emission was measured at 520 nm with excitation at 450 nm and 495 nm. The fluorescence excitation ratio at 495 nm and 450 nm ( $I_{495\text{ nm}}/I_{450\text{ nm}}$ ) was calculated, and endolysosomal pH in WT and Nuc1 astrocytes was measured to be  $\sim 4.5$  and  $5.7$ , respectively (\* $P = 0.031$ ). The elevated pH in Nuc1 homozygous astrocytes was restored to near normal by over-expression of  $\beta$ A3/A1-crystallin (\* $P = 0.026$ ). Empty vector had no effect. In all panels, graphs show mean values and error bars represent s.d. from a triplicate experiment representative of at least three independent experiments. Statistical analysis was performed by a two-tailed Student's t-test: \* $P < 0.05$ . Adapted with permission from Nature Communications.



**Fig. 12.**

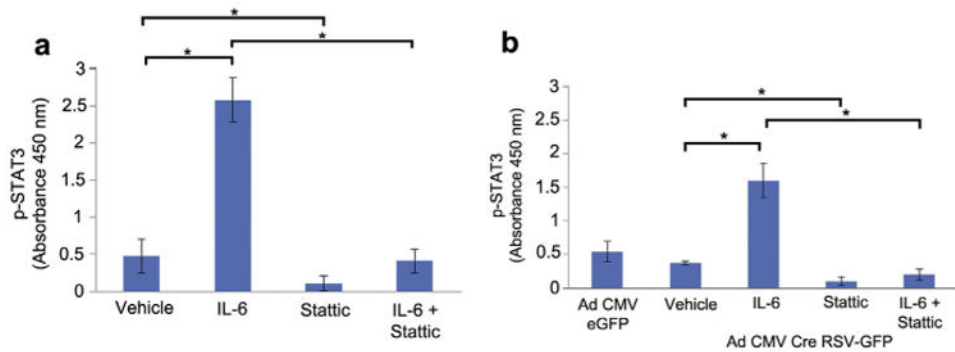
Intracellular processing and degradation of Notch receptor. a. WT and Nuc1 astrocytes transfected with myc-tagged full length Notch1 receptor were monitored for receptor clearance when co-cultured with astrocytes overexpressing Jagged1. Top panels show myc labeling (red) after transfection. Labeling decreased quickly in WT astrocytes, with little remaining after 3 h. Degradation was minimal in the Nuc1 astrocytes. Scale bar = 20  $\mu$ m. b. Cathepsin D activity was decreased in Nuc1 astrocytes to about 30% of the level in WT. Over-expression of  $\beta$ A3/A1-crystallin in Nuc1 astrocytes increased cathepsin D activity to 75% of WT level (\* $P = 0.037$ ). Graph shows mean values and error bars represent s.d. from a triplicate experiment representative of at least three independent experiments. Statistical analysis was performed by a two-tailed Student's t-test: \*\* $P < 0.01$ ; \* $P < 0.05$ . Adapted with permission from Nature Communications.



**Fig. 13.**

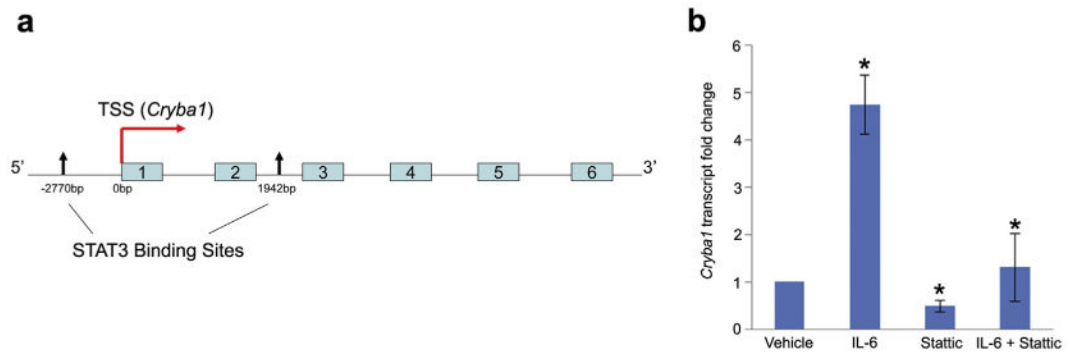
Impaired Notch signaling decreases VEGF secretion in astrocytes a. VEGF quantikine ELISA to detect levels of VEGF secreted into the medium showed significant reduction (~85%) in Nuc1 cells compared to WT cells. b. Treatment with the Notch inhibitor DAPT, significantly reduced secreted levels of VEGF in both WT (~60%) and Nuc1 (~75%) astrocytes compared to the respective vehicle-treated controls. c. Likewise, adenoviral *Cre*-recombinase-mediated knockdown of *Cryba1* in *Cryba1<sup>fl/fl</sup>* mouse astrocytes produced a similar reduction in VEGF secretion. Moreover, inhibition of Notch with DAPT further decreased VEGF secretion in both cultures. Error bars indicate s.d.; \*P < 0.05.

Adapted with permission from Scientific Reports.

**Fig. 14.**

$\beta$ A3/A1-crystallin modulates the phosphorylation of STAT3 in astrocytes. a. Analysis of p-STAT3 levels by ELISA revealed 5 fold induction of p-STAT3 in the presence of IL-6 and ~76% reduction in the presence of Stattic compared to the vehicle control. Stattic significantly decreased the levels of p-STAT3 in the presence of IL-6 (~85%) compared to the astrocytes treated with IL-6 alone. b. ELISA data revealed that IL-6 treatment induced p-STAT3 by 4.5 fold in *Cryba1* KD astrocytes compared to vehicle-treated astrocytes. Stattic decreased the level of p-STAT3 by ~80% when treated alone and by ~85% when treated in combination with IL-6 compared to vehicle-treated and IL-6 treated *Cryba1* KD astrocytes, respectively. Error bars indicate s.d.; \*P < 0.05.

Adapted with permission from Scientific Reports.

**Fig. 15.**

STAT3 regulates the expression of *Cryba1* in astrocytes. a. Schematic diagram of the mouse *Cryba1* gene showing the transcription start site (TSS) and the two STAT3 binding sites, one 2750 bp upstream of the start site (promoter region) and the other 1942 bp from the TSS in Intron 2. Exons are shown in boxes. b. Treatment of WT astrocytes with IL-6 resulted in 4.5 fold increase in the expression of *Cryba1* and Stattic treatment decreased the expression of *Cryba1* by ~51% compared to vehicle treated astrocytes. In astrocytes treated with both IL-6 and Stattic the expression of *Cryba1* was reduced by ~73% compared to astrocytes treated with IL-6 alone. Error bar indicate s.d.; \*P < 0.05.

Reproduced with permission from Scientific Reports.

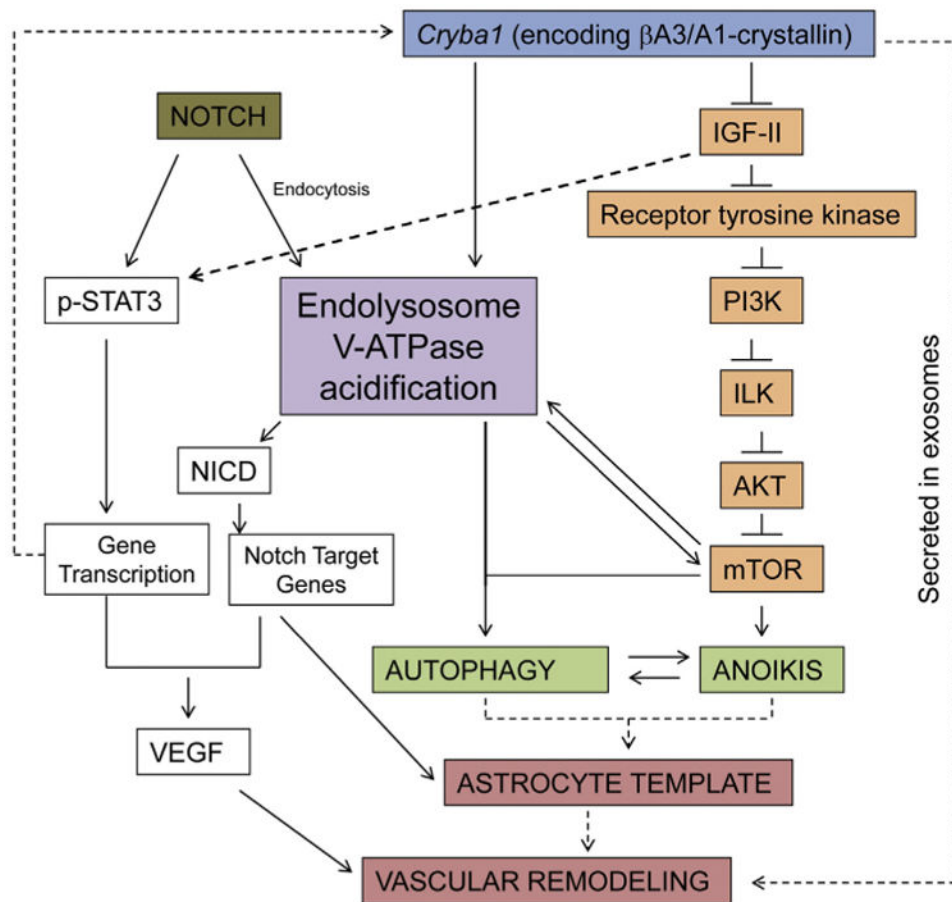


**Fig. 16.**

A schematic representation of signaling pathways and cellular processes modulated by  $\beta$ A3/A1-crystallin in astrocytes. It is likely that the protein regulates multiple processes and pathways in astrocytes by regulating V-ATPase and IGF-II. Solid lines denote links supported by experimental evidence and dashed lines are hypothetical. Abbreviations used: IGF-II, insulin-like growth factor-II; PI3K, phosphatidylinositol-3-kinase; ILK, integrin-linked kinase; mTOR, mechanistic target of rapamycin; V-ATPase, vacuolar-type  $H^+$ -ATPase; NICD, Notch intracellular domain, p-STAT3, phosphorylated Signal transducers and activators of transcription 3.